Molecular Precursors for the Electrodeposition of 2D-Layered Metal Chalcogenides for Next Generation Electronics

Philip N. Bartlett[1] (Email: P.N.Bartlett@soton.ac.uk), C. H. (Kees) de Groot[2], Victoria K. Greenacre[1],

Ruomeng Huang[2], Yasir J. Noori[2], Gillian Reid[1] (Email: G.Reid@soton.ac.uk) and Shibin Thomas[1]

1. *School of Chemistry, University of Southampton, Southampton SO17 1BJ, UK.*

2. *School of Electronics and Computer Science, University of Southampton, Southampton SO17 1BJ, UK.*

Abstract

Two-dimensional transition metal dichalcogenides (TMDCs) are highly anisotropic layered semiconductors, with general formula ME_2 (M = metal, E = sulfur, selenium or tellurium). Much current research focusses on TMDCs for catalysis and energy applications; they are also attracting great interest for next-generation transistor and optoelectronic devices. These high-tech applications place stringent requirements on the stoichiometry, crystallinity, morphology and electronic properties of mono-/few-layer materials. As a solution-based process, where the material grows specifically on the electrode surface, electrodeposition offers great promise as a readily-scalable, area-selective growth process. This review explores the state-of-the-art for TMDC electrodeposition, highlighting how the choice of precursor(s), solvent, with novel 'device-ready' electrode geometries, influence their morphologies and properties, thus enabling the direct growth of ultra-thin, highly anisotropic 2D TMDCs and much scope for future advances.

[H1] Introduction

Semiconductors are integral to modern technology and the chips that provide the processing power that drive the devices that modern society relies on, such as smartphones, tablets, and PCs. Each chip contains billions of semiconducting transistors. The demand for smaller, faster and lower power devices places an ever-increasing demand on the development of nanoscale semiconductors.

2D-Layered transition metal dichalcogenides (TMDCs) are an exciting class of highly tunable and anisotropic semiconductors with considerable promise for implementation into next generation electronic and optical devices with novel architectures.[1-5] TMDCs have the general formula, ME_2 (M = transition metal, especially Mo, W, Ti, Zr, Nb, Ta; E = chalogen, *i.e.* sulfur, selenium or tellurium) (Figure 1); the notation, MX_2, where X = chalcogen = S, Se, Te, is also used by some communities. They adopt

layered structures, and each of the monolayers consists of 2D hexagonally packed E-M-E structures (Figure 1a), where the metal atoms in the centre of the hexagonal plane are covalently bonded to the chalcogen atoms above and below this plane. In a TMDC each metal atom is coordinated by six chalcogens in either an octahedral or trigonal prismatic arrangement (Figure 1b). The monolayers are stacked through van der Waals (vdW) interactions to form bulk TMDCs, with the formation of a variety of polymorphs and polytypes dependant on the stacking sequence. The M-E-M bonding within the layers is strong (covalent), while there is weak E···E vdW bonding between the layers. These layered TMDCs exhibit extraordinary and unique layer-dependent physical properties when scaled down to thicknesses of only a few-layers, or even a single monolayer. Their unique combination of robust intra-layer bonds and weaker inter-layer bonding contributes to the distinct and highly anisotropic properties of TMDC materials. This means their electronic structures can be engineered through carefully controlling the number of layers, crystal phase, heterostructures and composition (for instance, the choice of metal and chalcogen). These versatile and highly tunable properties, together with the range of TMDCs that can exist, continue to attract a great deal of fundamental and technological research in fields ranging from electronics,[6-8] optoelectronics,[9-11] sensing[12] and catalysis,[13,14] to energy storage (batteries, supercapacitors)[15-18] and energy generation (photovoltaics, thermoelectric generators).[19-21]

Mechanical and liquid phase exfoliation (delamination from a bulk crystal) are commonly-used to prepare mono- and few-layer single crystalline TMDC flakes.[22,23] This approach has been instrumental in revealing the unique properties of TMDCs, including their light-matter interactions, and many of the novel electronic and optical device structures that have been demonstrated.[6,24] However, these methods are slow and require special care to avoid damage to the material, hence they are not suitable for producing devices on the scale necessary for mass-production in industry.

Production of mono-/few-layer TMDCs requires scalable and, ideally, area-selective **[G]** deposition techniques that deliver the TMDC only onto or into specific pre-patterned regions of a wafer substrate. Chemical vapour deposition (CVD),[25-27] atomic layer deposition (ALD),[28,29] and molecular beam epitaxy (MBE)[30,31] are currently the most common processing methods for the large-scale production of mono- and few-layer TMDCs. They can give high crystal quality, controllable thickness, and excellent electronic properties at full wafer-scale. A wide range of monolayer and thin film TMDCs, such as MoS_2, WS_2, WSe_2, VTe_2, have been obtained this way.[9,32] These methods have also been used to deposit TMDC heterostructures, such as WSe_2/MoS_2, $WSe_2/MoSe_2$ and MoS_2/WS_2.[33-35] However, they also have some drawbacks. For example, it is very challenging to grow large, single crystalline domain TMDC layers with these methods. This is because they typically produce multiple nuclei on the

2

substrate simultaneously, hence the as-deposited materials are polycrystalline; the crystallinity can be increased by annealing at high temperatures.

It is also important to note that these growth methods are (usually) not area-selective. For TMDCs grown on wafer-scale, various post-deposition processing steps, such as etching and patterning, are therefore required to create the necessary nanoscale dimensions and architectures.[36] Such processes are time-consuming, expensive and can introduce contamination and defects, which are detrimental to the material quality and functionality. The current processes that are carried out post-deposition to address this challenge have been the subject of an excellent review.[37] Advances in area-selective CVD and ALD for certain mono-layer TMDCs on lithographically-patterned substrates have also been reported.[38,39] However, there is considerable interest in developing novel TMDC growth methods capable of delivering high quality, patterned 2D-TMDC layers directly.

This article reviews the state-of the-art for the growth by electrodeposition of layered metal chalcogenide materials for semiconductor applications, with particular emphasis on the prospects for the scalable growth of ultrathin 2D TMDCs. Here, direct TMDC electrodeposition onto pre-defined regions of the substrate is of particular interest. For a discussion of the electrodeposition of semiconductor materials in general, the reader is directed to the reviews by Schlesinger *et al*[40] and Lincot.[41] A monograph on electrodeposition of a broader range of metal chalcogenides from across the periodic table is also available.[42] Among the most important considerations to deliver the precise stoichiometries, structures and morphologies, are the choice of the molecular precursor(s), the solvent, the nature and design of the electrode and the specific deposition parameters employed, each of which will be discussed. Developments in the use of single source precursors (SSPs) **[G]** (molecules or ions in which the directly bonded metal-chalcogen unit is already built-in), together with emerging work on the electrochemical growth of TMDCs from the edge of nano-band electrodes, are also highlighted.

[H1] Electrodeposition

Electrodeposition (also known as electroplating) is a technology that dates to the early 19th century and was first used to make printing plates and to apply decorative coatings such as silver plating on cutlery. Today it is often associated with large-scale engineering or decorative applications, such gold, nickel or chrome plating, with many thousands of electroplating businesses operating worldwide. It is widely used in printed circuit board manufacture, to grow thin films for the read heads in the manufacture of hard-disc storage drives[43] and to deposit metals and alloys. This application makes use of its ability to produce adherent, conformal coatings. Electrodeposition is also a key technology for

fabricating nano-scale electronics over 12-inch diameter wafers where it is the key step used to make the Cu interconnects and vias that wire up the (*ca.* 0.13 trillion) transistors in high-performance microprocessors through the Damascene process.[44]

[H2] Principles and criteria for electrodeposition

The choices of solvent, electrolyte **[G]** , salt and precursor for electrodeposition are governed by chemical constraints and there are often trade-offs that need to be made. There are important chemical factors that need to be considered when choosing the composition of the electrodeposition solution and in the design of precursor compounds. An excellent introduction to electrodeposition can be found in Paunovic and Schlesinger's book.[45]

First, the choice of solvent determines the accessible potential range and is important because it can act as a competitor ligand for the molecular precursor compound(s), leading to formation of additional coordination species in solution.[46] The purity of the solvent is crucial since small amounts of electroactive impurities can have a considerable effect.

Second, the choice of electrolyte has a significant effect. The electrolyte salt (C^+A^-) must not only dissolve in the solvent, but also dissociate to form mobile cations (C^+) and anions (A^-) so that the electrolyte solution is conducting. Its purity is again important because it is present at high (typically > 0.1 M) concentration. Many electrolytes are available, and their properties vary with the choice of cation and anion. For example, the choice of Cl^- as opposed to $[BF_4]^-$ or a fluorinated tetra-arylborate (BAr^F) anion, can have a considerable influence because of their differences in nucleophilicity. The choice of the electrolyte can also limit the potential range, since the anion or cation can undergo electrochemical oxidation or reduction (for example, at positive potential $Cl^- \rightarrow \frac{1}{2}Cl_2(g) + e^-$).

Third, the choice of precursor is also crucial. The chosen precursor compound(s) must be both soluble and stable in the electrolyte solution. Note that there can be ligand exchange, so there may be a mixture of coordination species in solution (speciation). For example, for $[N^nBu_4]_2[TeCl_6]$ dissolved in CH_2Cl_2 containing $[N^nBu_4]Cl$, the Te(IV) exists as a mixture of complex anions in equilibrium with the Cl^- anions from dissociation of $[N^nBu_4]Cl$ in the electrolyte solution.[47] This speciation can affect electrodeposition because the different complexes have different redox potentials and can have different electrochemical kinetics. The redox potential of the molecular precursor is an important factor – ideally it should be within the available potential range of the electrolyte solution so that electrodeposition is not accompanied by considerable electrochemical decomposition of the electrolyte. In general, this can be achieved through judicious choice of the ligands and the speciation of the precursor.[48]

130 Finally, the counter electrode [G] reaction also needs to be considered since an equal, but opposite,

131 current must be passing at the counter electrode. For aqueous solutions this can often be

132 accommodated by the evolution of oxygen gas which bubbles from the solution, but for non-aqueous

133 solutions and ionic liquids the counter electrode reaction needs more careful thought.

134 *[H2] Electrodeposition - an alternative route to TMDCs*

135 In comparison to CVD and ALD, in which the precursor species are delivered in the vapour phase (gas

136 phase) and the material growth is driven thermally, there has been much less work using

137 electrodeposition for the growth of 2D-TMDCs. However, electrodeposition offers a distinct set of

138 variables and parameters that can be optimised to control the growth of ultrathin, highly anisotropic

139 TMDC layers. Figure 2a illustrates the typical experimental set-up for electrodeposition using a three

140 electrode system, comprising a working electrode, counter electrode and reference electrode, to

141 maintain accurate control of the applied potential, along with indicative responses from some of the

142 electrochemical experiments that are most relevant to this area of work (Figures 2b-d). Figure 2e

143 shows a typical response from a chronoamperometric electrodeposition experiment, where the

144 current is monitored as a function of time.

145 Most importantly, electrodeposition is inherently a localised (area-selective) process, providing the

146 ability to grow the TMDC directly from a conductor into or onto a particular device architecture

147 precisely where required. This capability is extremely attractive for the production of new TMDC-

148 based nano-devices, as it would eliminate the need for post-deposition etching and patterning

149 processes.

150 There have been many papers on the electrodeposition of TMDC materials from aqueous (usually

151 acidic) electrolytes often containing a different precursor to deliver each of the metal and the

152 chalcogen. However, in general, the specific molecular species (ions and/or molecules) that exist in

153 these electrolytes have not been determined and so the actual reactive chemical species in the

154 electrolyte are usually not known.[49,50] As a result, the electrochemical processes that are observed

155 during TMDC electrodeposition are generally not thoroughly understood. Electrodeposition from

156 aqueous solution in these particular experiments also generally produces deposits that are irregular

157 and amorphous or polycrystalline. These are very suitable for (electro)catalysis, battery and super-

158 capacitor applications, which has been the motivation behind most of this work to-date.[51] For

159 example, in electrocatalytic water-splitting (the conversion of water into hydrogen and oxygen gas),

160 the presence of many nanocrystalline or amorphous TMDC particles is advantageous as the catalytic

161 reactions occur at defects and the edge sites of the 2D crystallites. However, these materials do not

display the highly anisotropic, extended 2D structures across the dimension scale (typically from a few nm^2 to tens of μm^2) required for future electronic and optical device applications.

In addition, aqueous electrolytes are inherently not well-suited for achieving fine control of 2D TMDC growth by electroreduction because of the generation of hydrogen gas, which dominates the voltammetric response at negative potentials. This can cause bubbles to form, and gives rise to a large, broad reduction wave in the voltammogram, which limits the potential window that can be used to drive the deposition of the TMDC itself.

When considering the fabrication of nano-devices using electrodeposition, the high surface tension of water can also hinder the penetration of aqueous electrolytes into high aspect-ratio structures. There are two other important considerations from a chemistry perspective. Firstly, the incompatibility of acidic aqueous media with many potential precursors, severely limiting the use of moisture-sensitive precursors that may otherwise be suitable for TMDC electrodeposition. Secondly, the Lewis basicity of water can lead to H_2O displacing one or more of the ligands present in the original precursor compound. This can cause the formation of multiple different species in the electrolyte solution, each of which will exhibit its own characteristic redox response. This is likely to result in more complicated electrochemical responses and loss of the potential-control necessary for growth of high quality 2D TMDC layers.

To explore 2D TMDCs for transistor and optical applications, several requirements need to be met to be able to deliver materials of sufficient quality. These include the need for large-scale production of single crystalline, mono-/few-layer TMDCs directly onto pre-patterned wafers, and control of the number and types of defects present. Other important considerations are the precise M:E ratio in the deposited material, the number of layers, and the ability to form heterostructures, since they will directly affect the functional properties of the TMDCs. Compatibility of the growth process with existing industrial manufacturing is also important if the process is to be adopted.

The high level of interest in these materials has also prompted efforts to explore alternative, complementary TMDC growth methods, including electrodeposition, to promote growth in the 2D plane. One reason for this is that precise control over heterostructure formation allows the development of hybrid devices that, for example, integrate sensing and computation components in one device,[52] or for optoelectronic devices, where it improves both the responsivity and the response time of photodetectors.[53]

[H2] Controlling morphology and crystallinity

6

Key considerations to achieve successful electrodeposition are the morphology and crystallinity of the deposit. The choice of deposition conditions (such as potential, mass transport, temperature, and concentration) will affect the morphology of the electrodeposited film and, in the case of the deposition of alloys or compounds (as opposed to pure elements), the composition of the deposit. The applied potential (which directly controls the energetic driving force for the deposition), and the mass transport conditions (for example stirring, or more controlled mass transfer using a rotating disc electrode, which replenishes the precursor concentration at the electrode) can be used to tune the structure of the generated TDMC. The mass transport in solution regulates the supply of the precursor molecules or ions and removal of any soluble by-products from the electrode surface. This can be important if there are coupled chemical reactions that are part of the overall electrodeposition process or where the ligands liberated during electrodeposition can change the local speciation at the electrode surface. For commercial plating baths it is not uncommon for specific technological developments that achieve the required outcomes to be developed on a trial and error basis.

A common approach to altering the morphology of electrodeposited films is to use additives. These are molecules that are added to the electrodeposition solution, generally at low concentration, that strongly adsorb on specific sites at the surface of the growing deposit and either inhibit or accelerate the local rate of deposition. Two common classes of additives are brighteners **[G]** and levellers **[G]**. Brighteners produce finely structured reflective deposits, whereas levellers reduce surface irregularities by slowing deposition on surface protrusions. Another common approach is to use pulsed deposition, in which the deposition potential is stepped between a high overpotential to favour the formation of many nucleation sites, followed by a lower overpotential to grow material on the nucleation sites at a slower rate. The control of electrodeposit morphology is a complex subject and is beyond the scope of this review. The reader is referred to the specialist literature for more details.[40]

[H2] Electrode materials and designs

In principle, a wide range of conducting materials can be used as substrates (electrodes) for electrodeposition. In practice, however, for fundamental electrochemical studies Pt, Au and glassy carbon electrodes are readily available and are most commonly used in the laboratory because they are convenient; they are robust, can be cleaned by polishing, and can be reused. For nano-electronic device applications, including metal chalcogenides, metals and alloys with high melting points and low reactivity that act as a diffusion barrier are preferred. This prevents migration (diffusion) of atoms or ions from the electrode into the deposit causing contamination. For nanodevice applications, TiN and carbon, in the form of graphene, are particularly suitable as these can be patterned using conventional nanofabrication processes. In the case of micro- and nano-fabricated structures, polishing of the

228 electrode surface, which is often undertaken in electrodeposition to reduce roughness and/or remove

229 surface impurities, is impractical and other cleaning methods (plasma cleaning, electrochemical

230 cleaning, *etc.*) must be used.

231 For fundamental studies of the voltammetry, disc electrodes, formed by encasing a wire or rod of the

232 electrode material in an insulating cylinder, are typically favoured since they have a well-defined

233 surface area and can be cleaned by polishing. These can be macroelectrodes **[G]** (diameter > 0.1 mm),

234 where mass transport is dominated by planar diffusion **[G]** (Figure 2b), microelectrodes **[G]** (diameter

235 < 50 μm), where radial diffusion **[G]** dominates (Figure 2c), and rotating disc electrodes, where the

236 rotation allows calculable and well-defined forced convective mass transport (Figure 2d). Of these, the

237 use of microelectrodes more closely corresponds to the mass transport conditions for deposition on

238 microfabricated structures. The use of microelectrodes also has the advantages of steady-state

239 diffusional mass transport and reduced *iR* drop **[G]** (reducing distortions in the electrochemistry

240 caused by poor control of the electrode potential as a result of high solution resistance), making them

241 a good choice for fundamental studies of the electrochemistry of the precursor compounds.[41]

242 For device applications, electrode structures are fabricated on planar substrates (typically commercial

243 12-inch Si wafers) using a range of standard cleanroom nanofabrication techniques to deposit and

244 pattern thin (10 – 100 nm) films of conductors and dielectrics. Industrially, electrodeposition

245 subsequently happens on a full-wafer scale, though in the research environment, the wafers are

246 usually diced before electrodeposition with limited further processing afterwards (see, for example

247 Ref. 41). Aggressive scaling down to nanoelectrodes and deposits is possible as the electrode

248 resistance and necessary current for electrodeposition scale identically, keeping a constant *iR* drop

249 independent of size.[56]

250 **[H1] Solvents and speciation**

251 A variety of solvents can be used for the electrodeposition of TMDCs and related layered metal

252 chalcogenides, from water to non-aqueous solvents (such as MeCN, DMF, DMSO, propylene

253 carbonate, CH_2Cl_2), to ionic liquids such as such as [bmim][BF_4] or [bmim][CF_3SO_3] (bmim = 1-butyl-3-

254 methylimidazolium),[57] and deep eutectic solvents, such as choline chloride/ethylene glycol.[58] Acidic

255 aqueous electrolytes and other protic solvents, like alcohols and glycols, are often used for

256 electroplating materials onto large area surfaces and there are many reports describing the

257 electrodeposition of various ME_2 (M = Zr, Mo, W; E = S, Se, Te) or M'_2E_3 (M' = Sb, Bi) materials from

258 acidic aqueous electrolytes. Typical metal precursors are sulfate salts, such as $Zr(SO_4)_2$,[59-62] and oxo-

259 anions, $[MoO_4]^{2-}$ [63-78] and $[WO_4]^{2-}$.[79-82] For the M'_2E_3 materials, metal halides such as $M'Cl_3$,[83-87] or oxo-

260 halides, M'OCl,[88-90] are often used. Typical chalcogen sources used in this area of work are Na_2S,

261 $[S_2O_3]^{2-}$, thiourea, SeO_2, $[SeO_3]^{2-}$, TeO_2 or $[TeO_3]^{2-}$. The majority of MoS_2 and WS_2 materials produced

by electrodeposition from aqueous solution have been for use in electrocatalytic water-splitting to generate hydrogen. For these processes the catalytic reactions take place on the exposed edges of the TMDC rather than on the vdW surfaces, so the rough, nanocrystalline or amorphous deposits, with many exposed edges, that are typically produced from these electrolyte baths are advantageous.

Turning to non-aqueous solvents, MeCN is one of the most commonly used non-aqueous solvents for electrochemical studies. However, it is important to be aware that MeCN can also act as a ligand, changing the speciation of the initial precursor, for example in:[91]

$$[Cu(H_2O)_x]^+ + n \text{ MeCN} \rightleftharpoons [Cu(MeCN)_n]^+ + x \text{ } H_2O$$
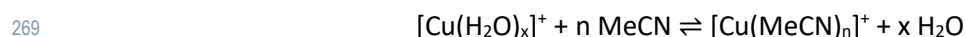
Thus, it is important to consider the effect of the choice of solvent on the speciation of the precursor. Room temperature ionic liquids (RTILs) and deep eutectic solvents have superseded water for the electrodeposition of some chalcogenide materials. Examples include, TiS_2 (from $TiCl_4$ and $Na_2[S_2O_3]$ in a choline chloride/urea eutectic),[92] and polycrystalline MoS_2[93] and Bi_2E_3[94] from RTILs. Theses solvents can have wide potential windows,[95,96] the option to access high electrodeposition temperatures (due to their high boiling points) and reduce the problems associated with H_2 evolution that occur during the deposition process from water and alcohols. However, ionic liquids can be difficult to purify sufficiently for use in electrodeposition and, like water, also exhibit relatively high surface tensions.[97]

When thinking about the choice of solvent and effects on speciation, it is useful to classify different solvents based on Kamlet and Taft's π^*, α and β parameters, where π^*, α and β describe the polarity, Lewis acidity [G] and Lewis basicity [G], respectively (Table 1).[98] Suitable solvents, should be polar ($\pi^* \geq 0.55$), aprotic ($\alpha \leq 0.2$), and weakly coordinating ($\beta \leq 0.2$).[99] This ensures that the electrolyte salt will dissociate sufficiently to make the solution conducting and that the solvent will not coordinate strongly with the precursor. The Taft solvent descriptors show that the commonly used non-aqueous solvents, such as DMSO, ethylene glycol and ionic liquids, are more Lewis basic than solvents such as CH_2Cl_2.

The so-called 'weakly-coordinating solvents',[99] such as CH_2Cl_2, generally have low donor-power. This reduces their tendency to compete as a ligand towards the dissolved precursors, leading to fewer different species in the electrolyte. They can be beneficial for the deposition of TMDCs, where the semiconducting behaviour is determined by the precise stoichiometry, structure, defect concentration and morphology of the material. When considering these alternative (aprotic) solvents, the electrochemical window of the solvent is a key factor, since this determines the potential range within which electrodeposition can be performed cleanly without introducing impurities from solvent degradation. The solvent donor properties also determine its compatibility with certain precursor compounds. MeCN, CH_2Cl_2 and supercritical CH_2F_2 have been used to facilitate the electrodeposition of various p-block elements, for example, elemental Te,[100] (sulfur-rich) WS_2 from $[NH_4]_2[WS_4]$,[101] mono- and few-layer TMDCs from SSPs, and ternary GeSbTe alloys from electrolytes containing multiple precursors.[102,103]

[H1] Molecular precursors

To identify suitable molecular precursors for the electrodeposition of metal chalcogenides from weakly coordinating solvents, several criteria need to be met. The precursor needs to be sufficiently soluble in the low polarity solvents and dissociation of precursor salts should occur to produce well-defined ions. Additionally, the reduction potentials for the precursor molecules/ions should be well-defined and accessible within the potential limits of the solvent electrolyte used. These will be dependent on the particular metal ion in the precursor, its oxidation state and the co-ligands present. The nature and fate of the ions and ligands that are liberated during the deposition process must also be considered to avoid undesirable chemical reactions in the electrolyte or precipitation of impurities during the deposition process.

This can be illustrated by considering the electrodeposition of elemental tellurium from $[N^nBu_4]_2[TeCl_6]$ salt in CH_2Cl_2 (Figure 3). The $[N^nBu_4]^+$ cation aids solubility of the salt in the low polarity CH_2Cl_2 solvent, and is not electrochemically active within the normal potential window of the solvent. Hence, this system has a cathodic potential limit that is suitable for observing the electroreduction of the $[TeCl_6]^{2-}$ anion. $[N^nBu_4]^+$ is also the same cation that is present in the $[N^nBu_4]Cl$ supporting electrolyte. As the elemental tellurium is deposited from the $[TeCl_6]^{2-}$ precursor, Cl^- anions are liberated and released into the solution; these are the same as the anion of the supporting electrolyte, therefore the ions present in the electrolyte do not change during the process.[104] It is important to note that the higher concentration of Cl^- at the electrode surface can alter the local speciation (e.g. in the Te case at low Cl^- electrolyte concentration) and this may change the chemistry of the electrodeposition reaction. This general strategy has been used successfully for the electrodeposition

of a wide range of p-block elements from CH_2Cl_2-based electrolytes, including Se, Te, Sb, Bi, Ga, In,[104] Sn,[105] and Pb.[106]

In some cases, different oxidation states of the p-block ion in the halometallate salt precursors can also be accessed by varying the synthesis procedure. For example, while Te(IV) is present in $[TeCl_6]^{2-}$, Te(II) can be incorporated in the form of $[TeI_4]^{2-}$.[47,107] Similarly, Ge(IV) can be incorporated in the form of $[GeCl_5]^-$ or $[GeCl_6]^{2-}$, whereas the $[GeX_3]^-$ anions (X = Cl, Br, I) contain Ge(II).[108] The choice of oxidation state and the nature of the halide ion (X^-) in the precursors also allow the electrochemical reduction potentials of the p-block halide ions to be tuned. This is particularly important when combinations of these salts are required to deposit a binary or ternary chalcogenide material.

For each of the p-block halometallate precursors above, when performing electroreduction to deposit the elemental form, the transfer of multiple electrons is required. For example, reduction of Te(IV) to Te(0) involves a four electron reduction. While the literature often implies that this occurs by *simultaneous* multi-electron reduction processes, in practice this is implausible based on Marcus theory.[109] The electroreduction of Te(IV) to Te(0) has been investigated in some detail by using a combination of electrochemical experiments in CH_2Cl_2, together with density functional theory calculations. This has led to a proposed catalytic process that involves the interaction of a coordinatively unsaturated Lewis acidic species ($[TeCl_5]^-$), produced via the equilibrium shown in Figure 3a, with the filled p-type orbitals projecting out from the surface of the growing Lewis basic Te(0) deposit (Figure 3b). It is proposed that this is followed by a sequence of one-electron transfer processes to cause 'stepwise reduction' to elemental tellurium, accompanied by liberation of further chloride ions from the tellurium.[47]

Two distinct strategies for molecular precursor development for the electrodeposition of metal chalcogenide materials from weakly coordinating solvents have been established. The first, and more commonly used to-date, uses 'multi-source precursors'. In this case, each element required for the target TMDC is delivered from a separate precursor compound. In the second approach both the metal and the chalcogen are bonded together and contained in a single molecular entity – 'single source precursors' (SSPs).

[H2] Electrodeposition using multi-source precursors

Electrodeposition of binary metal chalcogenides from multi-source precursors requires a combination of two different precursor compounds that form a chemically stable electrolyte, hence the compatibility of the individual salts in the solvent must also be considered. It has been found that combining the Bi(III) salt, $[N^nBu_4][BiCl_4]$, with the Te(IV) salt, $[N^nBu_4]_2[TeCl_6]$, in CH_2Cl_2 containing $[N^nBu_4]Cl$ supporting electrolyte forms a chemically stable electrolyte that allows the growth of the

target Bi_2Te_3 thin film semiconductor under electrochemical control.[1] In contrast, combining the Ge(II) salt, $[N^nBu_4][GeCl_3]$, with the same Te(IV) salt, $[N^nBu_4]_2[TeCl_6]$, in CH_2Cl_2, gives an unstable electrolyte that undergoes a spontaneous chemical reaction, precipitating elemental Te. This is most likely caused by the chemical oxidation of the Ge(II) (to Ge(IV)) by the Te(IV), which is itself reduced to Te(0). However, swapping to the Ge(IV) precursor, $[N^nBu_4][GeCl_5]$ (or a $[GeCl_6]^{2-}$ salt),[102,103] in combination with $[TeCl_6]^{2-}$ gives a stable multi-source electrolyte that can be used to electrodeposit germanium telluride under electrochemical control.

This approach has also proven to be remarkably effective for the deposition of various ternary alloys of GeSbTe onto TiN electrodes, which, although not a TMDC, is an important material for solid state memory applications, using a multi-source electrolyte containing $[GeCl_5]^-$, $[SbCl_4]^-$ and $[TeCl_6]^{2-}$ (Figure 4a).[102,103] In this case, the cyclic voltammetry shows distinct reduction waves for each of the three chlorometallate anions (Figure 4b). It is also possible to tune the composition of the alloy by adjusting both the relative ratios of the precursor salts in the electrolyte and by altering the reduction potential for the electrodeposition, allowing a range of alloy compositions to be accessed using this suite of precursors. This strategy has also been used for the deposition of functional GeSbTe alloys into a range of micro- and nano-patterned electrodes, by exploiting the area-selectivity inherent to electrodeposition. These materials were then investigated for application in solid state memory where their growth as thin films onto specific areas of pre-patterned arrays within geometrically constrained 3D nano- and micro-structures are advantageous for fast switching at low power and with high endurance.[111,112]


[H2] Electrodeposition using single source precursors

Since SSPs contain pre-formed M=E bonds, they can result in better-defined solution speciation in the electrolyte, as well as a simpler voltametric response, compared to multi-source precursors. This can be beneficial for the controlled growth of mono- and few-layer TMDCs, where precise control of the deposition conditions is advantageous.

Ammonium (NH_4^+) salts of $[MoS_4]^{2-}$ and $[WS_4]^{2-}$ are commercially available and have been the subject of intense research interest for the electrodeposition of MoS_2[113-133] and WS_2[134-136] onto various electrode arrangements from aqueous electrolytes. The $[NH_4]^+$ cations (or H_2O in aqueous electrodeposition) serve as the proton source to remove the excess sulfur (as H_2S). Typically, the as-deposited metal sulfides produced from the metal tetrathiolate precursors in aqueous electrolytes have stoichiometries considerably higher than the 1:2 ratio required for the deposition of the metal

12

disulfide and these can be converted to polycrystalline ME_2 by high temperature annealing. They have been produced by electrodeposition for a range of applications, including, electrocatalysis,[113,114,116,118,119,127,130] solar cells,[120,122] battery materials,[123] supercapacitors[129] and sensing.[117,124] However, these conditions generally produce deposits that are rough and irregular and therefore not well-suited for electronic or optical applications. $[MoE_4]^{2-}$ (E = S, Se) have also been used as SSPs to deposit dense amorphous nanoparticles of MoS_2 and $MoSe_2$ from an ionic liquid for hydrogen evolution catalysis.[137] The low costs associated with electrodeposition, coupled with its scalability, are particularly attractive for these applications.

The suitability of SSPs based on other $[MS_4]^{x-}$ anions (Figure 5a) is of interest to explore the versatility of this approach for electrodepositing other metal sulfide materials. For example, an aqueous $[NH_4][ReS_4]$ electrolyte has been implemented for the electrodeposition of ReS_2 onto 2D- and 3D-printed carbon electrodes for the photo-/electrochemical oxidation of water.[138] All of the $[ME_4]^{x-}$ precursors discussed so far produce the target metal chalcogenide under cathodic deposition (*via* electroreduction). In contrast, it has been shown that Schlippes salt, $Na_3[SbS_4] \cdot 9H_2O$, can be used as a SSP in aqueous alkaline solution to produce Sb_2S_3 films by anodic electrodeposition, according to the equation:

$$20\ H_2O + 2\ [SbS_4]^{3-} \rightarrow Sb_2S_3 + 5\ [SO_4]^{2-} + 40\ H^+ + 36\ e^-$$
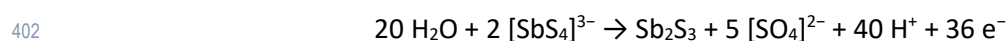
In this unusual case, the reduction of the Sb^{5+} to Sb^{3+} is accompanied by oxidation of the liberated sulfide to sulfate. Interest in Sb_2S_3 thin films arises from their resistive memory switching behaviour.[139]

As discussed, weakly coordinating solvents such as CH_2Cl_2 offers some advantages for TMDC electrodeposition compared to using water. However, the commercially available $[NH_4]_2[MS_4]$ (M = Mo, W) salts are poorly soluble in CH_2Cl_2. Therefore, it is necessary to change the $[NH_4]^+$ cation to an organic ammonium cation, such as $[N^nBu_4]^+$. The $[N^nBu_4]_2[MoS_4]$ salt exhibits good solubility in CH_2Cl_2, and studies on their suitability as SSPs have been very promising. The deposition of MS_2 from these sulfur-rich $[MS_4]^{2-}$ anions require the excess sulfur to be removed as H_2E. For the $[N^nBu_4]_2[MoS_4]$ precursor in CH_2Cl_2, this can be achieved by the addition of a small amount of an organic proton source, such as $[NMe_3H]^+$. This enables the cathodic deposition of amorphous $MoS_{2.3}$ thin films onto TiN electrodes, which are converted to crystalline 2D MoS_2 by annealing.[140] However, the breakdown of the proton source also occurs in a similar region to the $[MoS_4]^{2-}$ reduction and dominates features in the voltammetry, restricting the usable potential window in CH_2Cl_2 electrolytes. The reduction process for the analogous $[N^nBu_4]_2[WS_4]$ salt is completely masked by the peak associated with the breakdown of the $[NMe_3H]^+$ cation in the cyclic voltammogram, therefore WS_2 has not been obtained from this precursor.[141] Alternative SSPs for WS_2 are not available commercially.

13

Although they are not available commercially, the corresponding tetraselenometallate anions of Mo and W, $[MSe_4]^{2-}$, can be synthesised using established literature methods.[142,143] The $[N^nBu_4]_2[MSe_4]$ (M = Mo, W) salts also have good solubility in weakly coordinating solvents such as CH_2Cl_2. Analogy with the $[MoS_4]^{2-}$ ion, which is an effective SSP for MoS_2 electrodeposition, could suggest that the $[MoSe_4]^{2-}$ ion may be suitable as a SSP for the electrodeposition of 2D-layered $MoSe_2$ films. However, to achieve this, it will be necessary to identify an effective way to remove the excess selenium.

The need for a proton source to exploit these $[ME_4]^{2-}$ salts as SSPs has stimulated efforts to synthesise alternative precursors that contain the specific 1:2 metal:chalcogen ratio required for the target TMDC semiconductor, since this removes the need for the proton source and simplifies the electrochemistry. The tungsten(VI) sulfide chloride, $WSCl_4$, can be converted to the cis-$[WS_2Cl_4]^{2-}$ anion (Figure 5b), which was originally isolated as its $[PPh_4]^+$ salt,[144] and later as its $[NEt_4]^+$ salt for electrochemical studies.[141,] Thin films of WS_2 have been obtained by cathodic electrodeposition onto a TiN electrode, and further refinement of the experimental procedures allow 2D mono-and few-layer WS_2 growth from this tailored SSP. However, the corresponding tungsten selenide chloride salt, $[NEt_4]_2[WSe_2Cl_4]$, has not been isolated from $[WSeCl_4]$.[145] This is probably because the W=Se bonds are weaker than W=S bonds and therefore less stable. However, cathodic electrodeposition using the neutral $[WSeCl_4]$ as the SSP (Figure 5b), in MeCN with NEt_4Cl supporting electrolyte, produces very thin and smooth WSe_2 films.[146] Despite the 1:1 W:Se ratio in the precursor, production of the WSe_2 films does not require the addition of any further selenium source. It is proposed, therefore, that the deposition also involves Se atom transfer, according to the reaction:

$$2WSeCl_4 + 2e^- \rightarrow WSe_2 + WCl_6 + 2Cl^-$$

In the case of TMDC growth, the ability to deposit smooth, few- and mono-layer films is critical to unlock their electrical and optical properties. While one way of achieving ultra-thin TMDCs in electrodeposition is by controlling the deposition parameters, such as applied potential, time or charge passed, an alternative route to achieve this is by electropolishing of deposited TMDCs, through a top-down approach. Here, bulk TMDC materials could be thinned down to monolayers by electrochemically ablating the top layers in an acidic LiCl solution.[147] The electropolishing relies on the difference in activity of the edge sites and the relatively inert basal planes in the TMDCs, where the corrosion of materials begins at the edges of the multilayer flakes and gradually progresses towards the centre. Similar electropolishing strategies could be employed for electrodeposited TMDC films where the growth results in bulk multi-layered thin films. This technique, combined with electrodeposition, offers the prospect of an all-electrochemical pathway to achieve monolayer TMDCs.

14

[H1] 2D TMDC growth onto a conductor

SSPs compatible with non-aqueous, weakly-coordinating solvents tend to result in better-defined solution speciation, and, assuming that the deposition potential of the SSP is within the available potential window, allow TMDC films with well-controlled thicknesses to be electrodeposited onto a variety of electrode substrates. Electrodeposition, being an area-selective deposition method, offers growth control at the molecular scale by modulating the amount of charge passed during the deposition process. One of the challenges for ultra-thin (sub-5 nm) TMDC films is the choice of substrate. Since electrodeposition generally produces conformal coatings of the target material over electrically-defined surface features, classical metal or glassy carbon electrodes are not ideal as the variation in their surface roughness is large compared to the expected thickness of 2D TMDC films. This affects the film's morphology and layer-ordering. Monolayer graphene can be considered as an 'ideal' electrode substrate for TMDC growth as it is an atomically thin and extremely flat 2D conductor, therefore electrodeposition can occur on graphene without surface roughness issues.[148] Electrodepositing the TMDCs on directly on top of graphene can also be used to produce 2D TMDC on graphene heterostructures. By optimization of the deposition parameters, few-layer MoS_2/graphene heterostructures have been produced from the $[N^nBu_4]_2[MoS_4]$ precursor in dichloromethane.[149] This is a good example to demonstrate the nanoscale control that is possible using electrochemical techniques to produce ultra-thin TMDC films and heterostructures. Figure 6a illustrates a graphene electrode structure fabricated using the process in Figure 6b and implemented for ultra-thin TMDC growth using SSPs in CH_2Cl_2 electrolytes.[149] Further work has focussed on deposition of monolayer WS_2 on graphene. This was selected because the electrochemistry of the $[NEt_4]_2[WS_2Cl_4]$ precursor salt (1:2 W:S stoichiometry) is less complicated compared to the 1:4 Mo:S ratio in the $[N^nBu_4]_2[MoS_4]$ precursor. In the latter, the interference of the proton source (Me_3NHCl) is unavoidable. By controlling the time duration of the deposition, it has been possible to electrodeposit WS_2 monolayers onto patterned graphene electrodes, as illustrated in the transmission electron microscopy (TEM) image in Figure 6c.[150]

In addition to graphene, in principle, a semiconducting TMDC itself can be used as a substrate for electrodepositing a different TMDC material on top, to achieve vdW heterostructures. Electrodeposition offers a unique advantage here, as the TMDC heterostructures can be electrochemically deposited by simply switching the electrolyte solution. If the material quality is sufficiently high, this 2D heterostructure electrodeposition method could be extended to produce *p-n* junctions. An interesting target would be to deposit WSe_2 (*p*-type) on top of MoS_2 (*n*-type).

[H1] 2D TMDC growth over an insulator

As explained, traditionally, electrodeposition has been used to grow materials on top of conducting surfaces (electrodes). However, in the case of TMDCs, this prevents the direct electrical characterisation of the semiconductor material that is deposited, because the high conductivity of the electrode will dominate the electrical response. Moreover, depositing a semiconducting TMDC film on a conductor also limits the film's applications in electrical devices such as transistors. For these reasons, film transfer is required to enable electrical measurements of the electrodeposited TMDC films. Therefore, novel electrochemical techniques that enable the deposition of 2D materials onto insulating surfaces need to be developed.

One possible approach takes advantage of the strong anisotropy resulting from their 2D-layered structures, which helps to propagate the in-plane growth. This has been exploited to drive the TMDC growth over an insulating substrate (e.g. SiO_2) as illustrated in Figure 7. It has been achieved by constructing microelectrode structures, where the electrochemical growth starts at the ***edge*** of very thin nano-band electrodes **[G]** and progresses out from the electrode and over the insulator, as illustrated in the schematic in Figure 7a. Each individual electrode can be electrically-addressed separately, allowing deposition of one material (TMDC-1) from the left nano-band TiN electrode, and, if desired, a different material (TMDC-2) from the right side, as illustrated in Figures 7b-d. The clean-room processes required to fabricate these unusual electrode structures are shown in Figure 7e.[151] The rationale for this design is that since the tops of the electrode surfaces are covered by an insulator (SiO_2), only the extremely thin edges of the TiN nano-band electrodes (thickness sub-100 nm) are exposed to the electrolyte. Therefore, after nucleation onto the electrode edges under electrochemical control, growth progresses out over the insulating SiO_2 surfaces. This is promoted by the inherent 2D anisotropy of the TMDC. Using this nano-band electrode structure it has been shown that in-plane 2D growth of the MoS_2 across a 7 µm wide SiO_2 channel is around 20 times faster than the rate of inter-layer growth.[151] Figure 7f shows a TEM image of a region of tri-layer MoS_2 (after annealing) deposited in this way (i.e. where TMDC-1 = TMDC-2 = MoS_2). The amount of deposited material, and thereby the extent of 2D growth can be tuned by varying the precursor concentration, the duration of deposition or the quantity of charge passed during the deposition.

16

Using this nano-band electrode structure to drive the electrodeposition of the TMDC over the insulator therefore facilitates the deposition of ultrathin 2D TMDC films onto 'device-ready' substrates (suitable for developing 2D transistors). An additional advantage of the electrode configuration is that it enables the direct characterisation of the electrical properties of the resulting films, without film transfer. The current-voltage (*i-V*) measurements of the resulting MoS_2 films confirm the quality of the deposited MoS_2, which were later used to demonstrate photodetector devices.[151] Similar nano-band electrode structures have also been employed for the electrodeposition of WSe_2 from $[WSeCl_4]$ in MeCN,[146] resulting in smooth 2D WSe_2 thin films over the SiO_2 microchannels. This suggests that this is a versatile approach for the production of a range of ultra-thin TMDC semiconductors.

Nano-band electrodes could also provide a method for stacking 2D heterostructures, where the heterostructure can, for example, form a *p-n* junction, by growing different TMDCs from the left and right electrodes until the films overlap (Figure 7a). This can be achieved because each individual electrode shown in Figure 7b can be controlled separately so that the electrodeposition could be performed either simultaneously from both sides of the nano-band electrodes, or only from one side.

[H1] Conclusion and Outlook

Most of the existing literature on the electrodeposition of TMDCs has been focused on delivering TMDC materials suitable for (electro)catalytic and energy (solar cells, batteries, supercapacitors) applications, for which nanocrystalline or amorphous materials are ideal. Also, the majority of reports use aqueous electrolytes containing multi-source precursors to deliver the target TMDC. However, it has been shown that by using SSPs containing pre-formed metal-chalcogen bonds, in combination with weakly coordinating solvents, where the solution speciation of the precursor is well-defined, allows more precise control of the deposition potential and the material growth. Therefore, the controlled electrochemical growth of ultrathin 2D-layered TMDCs is an emerging area of research with good prospects for the scalable production of TMDCs for electrical and optical applications. Notably, compared to CVD, where there has been a huge amount of work done, electrodeposition of 2D TMDCs is still at the early stages of development, but we anticipate a considerable increase in research

17

interest in this area in the coming years. A key remaining challenge is that the range of molecular SSPs with the necessary characteristics to specifically promote in-plane 2D TMDC growth is currently limited. Therefore, new developments in inorganic synthesis are necessary to produce novel SSPs to improve control of the TMDC material quality further and to extend the range of TMDCs that can be electrodeposited. This will allow tuning of the electrical and optical properties for particular target applications. For example, smooth 2D NbS_2 and $NbSe_2$ films are interesting targets due to their intriguing magnetic properties, while transition metal ditellurides from SSPs are yet to be realised. A recent review of transition metal chalcogenide halide chemistry may offer routes for other possible SSPs.[152] The precursor choice may also enable band-gap tuning.

Realising the potential of this emerging area requires further optimization of both the molecular precursors to deliver the ME_2 layers and the electrodeposition process and conditions to form uniform, high quality, single crystalline 2D-layered TMDCs, without the need to anneal post-deposition. This will require fundamental studies of the deposition mechanisms involved, including the electrolyte solution speciation, the electrolyte-electrode interfaces, and the electrochemically-driven deposition mechanisms. Hence, this is the second area where much new research is needed, through a combined approach bringing together experimental work (precursor synthesis and electrochemistry) and computational studies. Specifically, current computational work on electrocatalytic H_2 evolution from TMDCs needs to be extended to DFT calculations of the precursor solutions. This can then be combined with calculations on electrolyte/electrode interactions and the individual deposition steps to provide further mechanistic insights. Performing the electrodeposition at elevated temperatures may also increase the TMDC crystallinity because it increases the mobility of intermediates on the growing TMDC surface and the rates of associated chemical reactions such as ligand exchange or dissociation. To achieve this, other possible solvents with suitable solvent parameters and higher boiling points could be employed.[153]

Optimisation of the anisotropic (in-plane) growth **[G]** may be achieved by looking for molecular additives that adsorb onto the chalcogenide surface of the growing TMDC inhibiting multilayer growth in favour of monolayer growth. In the case of 2D TMDC growth over an insulator, the use of an insulating layer of hexagonal boron nitride matching the TMDC hexagonal structure may be beneficial. Electrochemical polishing also affords a possible way to thin electrochemically deposited multi-layer TMDCs down to mono- or few-layer samples.[147]

To electrodeposit 2D materials with the electronic and optical characteristics necessary for novel devices it will be important to find ways to control the doping levels so that *n*-type and *p*-type materials can be produced. This may be possible through the addition of very small amounts of a

chalcogen source to the electrolyte solution. Controlling the nucleation and growth will also be very important for producing high quality ohmic contacts.

In principle, electrodeposition can also provide sufficiently precise control for monolayer-by-monolayer growth of TMDC vertical heterostructures with sharp interfaces by switching the electrolyte solution, similar to the electrochemical atomic layer deposition (EALD) method reported by Stickney and co-workers for germanium antimony telluride films,[154] or by the Schwarzacher group for ultrathin layer-by-layer growth of metallic multilayers for magnetic materials.[155,156] These provide interesting lines of inquiry for exploiting electrodeposition towards future TMDC-based nanoelectronic and photonic devices. Increasing understanding of how the precursor chemistry influences the deposition process will be critical for all of these.

Looking forward, as the molecular precursor chemistry evolves, the ability to achieve a controlled compositional gradient or a modulated composition within a single TMDC monolayer may be possible. This may be achieved by exploiting the 2D growth from a nano-band electrode design and adjusting the electrochemical potential during monolayer growth. For example, it may be possible to vary the composition of $MoS_{2-x}Se_x$ within a single monolayer. This might be achieved by combining two SSPs with different redox potentials, one for monolayer MoS_2 electrodeposition the other for $MoSe_2$ growth, in the same solution at appropriate concentrations Then, by altering the potential and/or solution composition during the deposition process, drive the growth of one material or the other. Electrodeposition is uniquely suited for this because one precursor solution can be swapped to a different one very easily.

Acknowledgements

Author contributions

P.N.B. and G.R. conceived the idea and drafted the proposal. P.N.B., R.H., S.T. and G.R. wrote most of the content. Y.J.N., C.H.D.G., R.H., V.K.G. and S.T. prepared the graphic concepts. All of the authors edited and revised the manuscript.

Competing interests

The authors declare no competing interests.

References

1) Chowdhury, T., Sadler, E. C. & Kempa, T. J., Progress and Prospects in Transition-Metal Dichalcogenide Research Beyond 2D. *Chem. Rev.* **120**, 12563–12591 (2020).

2) Manzeli, S., Ovchinnikov, D., Pasquier, D., Yazyev, O. V. & Kis, A., 2D transition metal dichalcogenides. *Nature Rev. Mater.* **2**, 17033 (2017).

3) Yin, X. *et al*, Recent developments in 2D transition metal dichalcogenides: phase transition and applications of the (quasi-)metallic phases. *Chem. Soc. Rev.* **50**, 10087-10115 (2021).

4) Choi, W., Choudhary, N., Han, G. H., Park, J., Akinwande, D. & Lee, Y. H., Recent development of two-dimensional transition metal dichalcogenides and their applications. *Mater. Today*, **20**, 116-130 (2017).

5) Chhowalla, M., Shin, H. S., Eda, G., Li, A.-J., Loh, K. P. & Zhang, H., The chemistry of two-dimensional layered transition metal dichalcogenide nanosheets. *Nature Chem*. **5**, 263-375 (2013).

6) Wang, Q. H., Kalantar-Zadeh, K., Kis, A., Coleman, J. N. & Strano, M. S., Electronics and optoelectronics of two-dimensional transition metal dichalcogenides. *Nature Nanotech*. **7**, 699-712 (2012).

7) Wu, F. *et al*, Vertical MoS_2 transistors with sub-1-nm gate lengths. *Nature,* **603**, 259–264 (2022).

8) Lin, Z. *et al*, Solution-processable 2D semiconductors for high-performance large-area electronics. *Nature,* **562**, 254–258 (2018).

9) Xia, F., Wang, H., Xiao, D., Dubey, M. & Ramasubramaniam, A., Two-dimensional material nanophotonics. *Nature Photon.* **8**, 899–907 (2014).

10) Massicotte, M. e*t al*, Picosecond photoresponse in van der Waals heterostructures. *Nature Nanotech.* **11**, 42–46 (2016).

11) Yu, W. J. *et al*, Highly efficient gate-tunable photocurrent generation in vertical heterostructures of layered materials. *Nature Nanotech.* **8**, 952–958 (2013).

12) Barua, S., Dutta, H. S., Gogoi, S., Devi, R. & Khan, R., Nanostructured MoS_2-Based Advanced Biosensors: A Review. *ACS Appl. Nano Mater.* **1**, 2–25 (2018).

13) Voiry, D., Yang, J. & Chhowalla, M., Recent Strategies for Improving the Catalytic Activity of 2D TMD Nanosheets Toward the Hydrogen Evolution Reaction. *Adv. Mater*. **28**, 6197-6206 (2016).

14) Yin, J. *et al*, Optimized Metal Chalcogenides for Boosting Water Splitting. *Adv. Sci.* **7**, 1903070 (2020).

15) Lei, Z., Zhan, J. Tang, L., Zhang, Y. & Wan, Y., Recent Development of Metallic (1T) Phase of Molybdenum Disulfide for Energy Conversion and Storage. *Adv. Energy Mater*. **8**, 1703482 (2018).

16) Ma, Q. *et al*, 2D Materials for All-Solid-State Lithium Batteries. *Adv. Mater.* **34**, 2108079 (2022).

17) Wang, Z. *et al*, Unveiling highly ambient-stable multilayered 1T-MoS_2 towards all-solid-state flexible supercapacitors. *J. Mater. Chem. A,* 7, 19152-19160 (2019).

18) Acerce, M., Voiry, D. & Chhowalla, M., Metallic 1T phase MoS_2 nanosheets as supercapacitor electrode materials. *Nature Nanotech.* **10**, 313-318 (2015).

19) Nazif, K. N. *et al*, High-specific-power flexible transition metal dichalcogenide solar cells. *Nature Commun.* **12**, 7034 (2021).

20) Pang, H. *et al*, Realizing N-type SnTe Thermoelectrics with Competitive Performance through Suppressing Sn Vacancies. *J. Am. Chem. Soc.* **143**, 8538–8542 (2021).

21) Sethi, V. *et al*, Tungsten dichalcogenide $WS_{2x}Se_{2-2x}$ films *via* single source precursor low-pressure CVD and their (thermo-)electric properties. *J. Mater. Chem. A*, **11**, 9635-9645 (2023).

22) Raza, A. *et al*, Advances in Liquid-Phase and Intercalation Exfoliations of Transition Metal Dichalcogenides to Produce 2D Framework. *Adv. Mater. Interfaces*, **8**, 2002205 (2021).

23) Zhang, Q., Mei, L., Cao, X., Tang, Y. & Zeng, Z., Intercalation and exfoliation chemistries of transition metal dichalcogenides. *J. Mater. Chem. A*, 8, 15417–15444 (2020).

24) Busch, R. T. *et al*, Exfoliation procedure-dependent optical properties of solution deposited MoS_2 films. *npj 2D Mater. Appl.* **7**, 12 (2023).

25) Wang, J. *et al*, Controlled growth of atomically thin transition metal dichalcogenides via chemical vapor deposition method. *Mater. Today Adv*. **8**, 100098 (2020).

26) Hoang, A. T., Qu, K., Chen, Z & Ahn, J.-H., Large-area synthesis of transition metal dichalcogenides *via* CVD and solution-based approaches and their device applications. *Nanoscale*, **13**, 615-633 (2021).

27) Li, H., Li, Y., Aljarb, A., Shi Y. & Li, L.-J., Epitaxial Growth of Two-Dimensional Layered Transition-Metal Dichalcogenides: Growth Mechanism, Controllability, and Scalability. *Chem. Rev.* **118**, 6134–6150 (2018).

28) Mattinen, M, Leskelä, M. & Ritala, M., Atomic Layer Deposition of 2D Metal Dichalcogenides for Electronics, Catalysis, Energy Storage, and Beyond. *Adv. Mater. Interfaces*, **8**, 2001677 (2021).

29) Cho, A.-H. et al, Stepwise growth of crystalline MoS_2 in atomic layer deposition. *J. Mater. Chem. C*, **10**, 7031-7038 (2022).

30) Singh, D. K. & Gupta, G., van der Waals epitaxy of transition metal dichalcogenides *via* molecular beam epitaxy: looking back and moving forward. *Mater. Adv.* **3**, 6142-6156 (2022).

31) Choudhury, T. H., Zhang, X., Al Balushi, Z. Y., Chubarov, M. & Redwing, J. M., Epitaxial Growth of Two-Dimensional Layered Transition Metal Dichalcogenides. *Ann. Rev. Mater. Res*. **20**, 155-177 (2020).

32) Li, J. *et al*, Synthesis of Ultrathin Metallic MTe_2 (M = V, Nb, Ta) Single-Crystalline Nanoplates. *Adv. Mater.* **30,** 1801043 (2018).

33) Gong, Y. *et al*, Two-Step Growth of Two-Dimensional WSe_2/$MoSe_2$ Heterostructures. *Nano Lett.* **15**, 6135–6141 (2015).

34) Li, M. Y. *et al*, Epitaxial growth of a monolayer WSe_2-MoS_2 lateral p-n junction with an atomically sharp interface. *Science*, **349**, 524-528 (2015).

35) Zhou, J. *et al*, Morphology Engineering in Monolayer MoS_2-WS_2 Lateral Heterostructures. *Adv. Funct. Mater.* **28**, 1801568 (2018).

36) Giri, A.; Park, G. & Jeong, U. Layer-Structured Anisotropic Metal Chalcogenides: Recent Advances in Synthesis, Modulation, and Applications. *Chem. Rev.* **123**, 3329-3442 (2023).

This article provides a detailed review of the various processes typically used to grow 2D TMDCs and the modulation of the films for various applications.

37) Zhou, H., Zhang, C., Gao, A., Shi, E., Guo, Y., Patterned growth of two-dimensional atomic layer semiconductors, *Chem. Commun*. **60**, 943-955 (2024).

This work sets out the current state-of-the-art for patterning 2D semiconductors on the nanoscale.

38) Balasubramanyam, S.; Merkx, M. J. M.; Verheijen, M. A.; Kessels, W. M. M.; Mackus, A. J. M. & Bol, A. A., Area-selective atomic layer deposition of two-dimensional WS$_2$ nanolayers. *ACS Materials Lett.* **2**, 511-518 (2020).

39) Parsons, G. N. & Clark, R. D., Area-selective deposition: fundamentals, applications, and future outlook. *Chem. Mater*. **32**, 4920-4953 (2020).

This article provides a review of area-selective deposition of 2D materials, with a particular focus on CVD and ALD techniques.

40) Schlesinger, T. E.; Rajeshwar, K. & de Tacconi, N. R. Electrodeposition of Semiconductors. In *Modern Electroplating*; Schlesinger, M., Ed.; Springer: New York, Chapter 14, pp 383–411 (2010).

41) Lincot, D., Electrodeposition of semiconductors. *Thin Solid Films*, **487**, 40-48 (2005).

42) Bouroushian, M., Electrochemistry of Metal Chalcogenides. *Monographs in Electrochemistry*, Ed. Scholtz, F., Springer, Heidelberg (2010).

43) Osaka, T., Electrodeposition of highly functional thin films for magnetic recording devices of the next century*, Electrochim. Acta,* **45**, 3311-3321 (2000).

44) Andricacos, P. C., Uzoh, C., Dukovic, J. O., Horkans, J. & Deligianni, H., Damascene Copper electroplating for chip interconnections, *IBM J. Res, Develop.* **42**, 568-574 (1998).

45) Fundamentals of Electrochemical Deposition Second Edn, (Eds. Paunovic, M. & Schlesinger, M.), Wiley, ISBN 0-471-71221-3, 373 (2006).

This book provides a very useful introduction to the principles of electrodeposition.

46) Black, A. W. & Bartlett, P. N., Selection and characterisation of weakly coordinating solvents for semiconductor electrodeposition. *Phys. Chem. Chem. Phys*. **24**, 8093-8103 (2022).

47) Cook, D. A. et al, Tellurium electrodeposition from tellurium(II) and tellurium(IV) chloride salts in dichloromethane. *Electrochim. Acta*, **456**, 142456 (2023).

48) Bartlett, P. N., Cummings, C. Y., Levason, W., Pugh, D. & Reid, G., Halometallate Complexes of Germanium(II) and (IV): Probing the Role of Cation, Oxidation State and Halide on the Structural and Electrochemical Properties, *Chem. Eur. J*. **2**, 5019-5027 (2014).

49) Aliyev, A. S.; Elrouby, M. & Cafarova, S. F., Electrochemical synthesis of molybdenum sulfide semiconductor. *Mater. Sci. Semicond. Processing*, **32**, 31-39 (2015).

50) Zhang, L.; Wu, L.; Li, J. & Lei, J., Electrodeposition of amorphous molybdenum sulfide thin film for electrochemical hydrogen evolution reaction. *BMC Chemistry*, **13**, 88 (2019).

51) Mohapatra, S., Das, H. T., Tripathy, B. C., Das, N., Recent Developments in Electrodeposition of Transition Metal Chalcogenides-Based Electrode Materials for Advance Supercapacitor Applications: A Review, *Chem. Rec*. **24**, e202300220 (2024).

52) Zhang, Z., Wang, S., Liu, C., Xie, R., Hu, W. & Zhou, P., All-in-one two-dimensional retinomorphic hardware device for motion detection and recognition. *Nature Nanotech*. **17**, 27–32 (2022).

53) Shin, G, H., Park, C., Lee, K. J., Jin, H. J. & Choi, S. Y., Ultrasensitive Phototransistor Based on WSe_2–MoS_2 van der Waals Heterojunction. *Nano Lett.* **20**, 5741–5748 (2020).

54) Schlesinger, M. & Paunovic, M., Modern Electroplating, John Wiley & Sons, Inc. (2010).

55) Reeves, S. J., Noori, Y. J., Zhang, W., Reid, G. & Bartlett, P. N., Chloroantimonate electrochemistry in dichloromethane, *Electrochim. Acta*, **354**, 136692 (2020).

56) Huang, R. *et al*, Towards a 3D GST phase change memory with integrated selector by non-aqueous electrodeposition. *Faraday Disc.* **213**, 339–355 (2019).

57) Szymczak, J., Legeai, S., Michel, S., Diliberato, S., Stein, N. & Boulanger, C., Electrodeposition of stoichiometric bismuth telluride Bi_2Te_3 using a piperidinium ionic liquid binary mixture, *Electrochim. Acta,* **137**, 586594 (2014).

58) Hansen, B. B. et al, Deep Eutectic Solvents: A Review of Fundamentals and Applications, *Chem. Rev.* **121**, 1232−1285 (2021).

59) Sargar, A. M., Patil, N. S., Mane, S. R., Gawale, S. N. & Bhosale, P. N., Optostructural and electrical studies on electrodeposited Indium doped ZrS_2 thin films. *J. Alloys Cmpds*. **474**, 14-17 (2009).

60) Hankare, P. P. *et al*, Effect of annealing on properties of $ZrSe_2$ thin films. *J. Crystal Growth*, **294**, 254-259 (2006).

61) Sargar, A. M., Patil, N. S., Mane, S. R., Gawale, S. N. & Bhosale, P. N., Electrochemical Synthesis and Characterisation of $ZrSe_2$ Thin Films. *Int. J. Electrochem. Sci.* **4,** 887-894 (2009).

62) Rakkini, A. P. V. & Mohanraj, K., Influence of pH of the electrolyte on the formation and properties of electrodeposited $ZrSe_2$ thin films. *Inorg. & Nano Met. Chem*. **52**, 570-575 (2022).

63) Manyepedza, T., Courtney, J. M., Snowden, A., Jones, C. R. & Rees, N. V., Impact Electrochemistry of MoS_2: Electrocatalysis and Hydrogen Generation at Low Overpotentials. *J. Phys. Chem. C*, **126**, 17942–17951 (2022).

64) Teli, A. M. *et al***,** Electrodeposited crumpled MoS_2 nanoflakes for asymmetric supercapacitor, *Ceram. Mater*. **48**, 29002-29010 (2022).

65) Strange, L. E., Garg, S., Kung, P., Ashaduzzaman, M., Szulczewski, G. & Pan, S., Electrodeposited Transition Metal Dichalcogenides for Use in Hydrogen Evolution Electrocatalysts. *J. Electrochem. Soc.* **169**, 026510 (2022).

66) Soram, B. S., Dai, J. Y., Thangjam, I. S., Kim, N. H. & Lee, J. H., One-step electrodeposited MoS_2@Ni-mesh electrode for flexible and transparent asymmetric solid-state supercapacitors. *J. Mater. Chem. A*, **8**, 24040-24052 (2020).

67) Mabayoje, O. *et al*, Electrodeposition of MoS_x Hydrogen Evolution Catalysts from Sulfur-Rich Precursors. *ACS Appl. Mater. Interfaces,* **11**, 32879–32886 (2019).

68) Li, C.-D., Wang, W.-W., Jin, M., Shen, Y. & Xu, J.-J., Friction Property of MoS_2 Coatings Deposited on the Chemical-Etched Surface of Al–Si Alloy Cylinder Liner. *J. Tribol.* **140,** 041302 (2018).

69) Quy, V. H. V. *et al*, Electrodeposited MoS₂ as electrocatalytic counter electrode for quantum dot- and dye-sensitized solar cells. *Electrochim. Acta*, **260**, 716-725 (2018),

70) Erfanifan, S. *et al*, Tunable bandgap and spin-orbit coupling by composition control of MoS₂ and MoO$_x$ (x = 2 and 3) thin film compounds. *Mater. & Des.* **122**, 220-225 (2017).

71) Anand, T. J. S., Sanjeeviraja, C. & Jayachandran, M., Preparation of layered semiconductor (MoSe₂) by electrosynthesis. *Vacuum*, **60**, 431-435 (2001).

72) Ponomarev, E. A., Neumann-Spallart, M., Hodes, G. & Lévy-Clément, C., Electrochemical deposition of MoS₂ thin films by reduction of tetrathiomolybdate. *Thin Solid Films,* **280**, 86-89 (1996).

73) Poorahong, S., Izquierdo, R. & Siaj, M., An efficient porous molybdenum diselenide catalyst for electrochemical hydrogen generation. *J. Mater. Chem. A*, **5**, 20993-21001 (2017).

74) Kowalik, R., Kutyła, D., Mech, K., Żabinski, P., Wróbel, M. & Tokarski, T., Electrochemical Deposition of Mo-Se Thin Films. *ECS Trans.* **64,** 23 (2015).

75) Dukstiene, N., Kazancev, K., Prosycevas, I. & Guobiene A., Electrodeposition of Mo-Se thin films from a sulfamatic electrolyte. *J. Sol. St. Electrochem.* **8,** 330-336 (2004).

76) Kim, E.-K. *et al*, Epitaxial electrodeposition of single crystal MoTe₂ nanorods and Li⁺ storage feasibility. *J. Electroanal. Chem*. **878**, 114672 (2020).

77) Myung, N. *et al*, Electrosynthesis of MoTe₂ Thin Films: A Combined Voltammetry-Electrochemical Quartz Crystal Microgravimetry Study of Mechanistic Aspects. *J. Electrochem. Soc.* **167** 116510 (2020).

78) Zhou, Y., Jia, L. Feng, Q., Wang, T., Li, X. & Wang, C., MoTe₂ nanodendrites based on Mo doped reduced graphene oxide/polyimide composite film for electrocatalytic hydrogen evolution in neutral solution. *Electrochim. Acta*, **229**, 121-128 (2017).

79) Veeralingam, S., Durai, L. & Badhulika, S., Facile Fabrication of P(Electrodeposition)/N(Solvothermal) 2D-WS₂-Homojunction Based High Performance Photo Responsive, Strain Modulated Piezo-Phototronic Diode. *ChemNanoMat*, **5,** 1521-1530 (2019).

80) Devadasan, J. J., Sanjeeviraja, C. & Jayachandran, M., Electrodeposition of p-WS₂ thin film and characterisation. *J. Cryst. Growth,* **226**, 67-72 (2001)**.**

81) Delphine, S. M., Jayachandran, M. & Sanjeeviraja, C., Pulsed electrodeposition and characterisation of tungsten diselenide thin films. *Mater. Chem. Phys.* **81**, 78-83 (2003).

82) Devadasan, J. J., Sanjeeviraja, C. & Jayachandran, M., Electrosynthesis and characterisation of n-WSe₂ thin films. *Mater. Chem. Phys*. **77**, 397-401 (2003),

83) Peng, Z. *et al*, Controllable (h k l) preferred orientation of Sb₂S₃ thin films fabricated by pulse electrodeposition. *Sol. Energy Mater. Sol. Cells*, **253**, 112208 (2003).

84) García, R. G. A., Cerdán-Pasarán, A., Perez, E. A. R., Pal, M., Hernández, M. M. & Mathews, N. R., Phase pure CuSbS₂ thin films by heat treatment of electrodeposited Sb₂S₃/Cu layers. *J. Sol. St. Electrochem.* **24**, 185–194 (2020).

85) Garcia, R. G. A., Avendaño, C. A. M., Pal, M., Delgado, F. P. & Mathews, N. R., Antimony sulfide (Sb₂S₃) thin films by pulse electrodeposition: Effect of thermal treatment on structural, optical and electrical properties. *Mater. Sci. Semicond. Proc.* **44**, 91-100 (2016).

86) Subramanium, S. *et al*, High-energy ion induced physical and surface modifications in antimony sulphide thin films. *Curr. Appl. Phys.* **10**, 1112-1116 (2010).

87) Yesugade, N. S., Lokhande, C. D. & Bhosale, C. H., Structural and optical properties of electrodeposited Bi_2S_3, Sb_2S_3 and As_2S_3 thin films. *Thin Solid Films*, **263**, 145-149 (1995).

88) Majidzade, V. A., Javadova, S. P., Jafarova, S. F., Aliyev, A. S. & Tagiyev, D. B., Electrochemical Deposition of Sb_2S_3 Thin Films. Russ. J. Appl. Chem. 95, 1627–1633 (2022).

89) Majidzade, V. A., Aliyev, A. S., Guliyev, P. H. & Babanly, D. M., Electrodeposition of the Sb_2Se_3 thin films on various substrates from the tartaric electrolyte. *J. Electrochem. Sci. Eng.*, **10**, 1–9 (2020).

90) Majidzade, V. A., Aliyev, A. S., Qasimogli, I., Quliyev, P. H. & Tagiyev, D. B., Electrical Properties of Electrochemically Grown Thin Sb_2Se_3 Semiconductor Films. *Inorg. Mater.,* **55**, 979–983 (2019).

91) MacLeod, D., Parker, A. J. & Singh, P., Electrochemistry of copper in aqueous acetonitrile, *J. Soln. Chem.* **10**, 757-774 (1981).

92) Asif, O., Azadian, F. & Rastogi, A. C., Titanium Disulphide (TiS_2) Dichalcogenide Thin Films as Inorganic Hole Transport Layer for Perovskite Solar Cells Synthesized from Ionic Liquid Electrodeposition, *MRS Adv*. **5**, 3555-3564 (2020).

93) Murugesan, S, Akkineni, A., Chou, B. P., Glaz, M. S., Vanden Bout, D. A. & Stevenson, K. J., Room Temperature Electrodeposition of Molybdenum Sulfide for Catalytic and Photoluminescence Applications. *ACS Nano*, **7**, 8199-8205 (2013).

94) Szymczak, J., Legeai, S., Michel, S., Diliberato, S., Stein, N. & Boulanger, C., Electrodeposition of stoichiometric bismuth telluride Bi_2Te_3 using a piperidinium ionic liquid binary mixture*, Electrochim. Acta,* **137**, 586594 (2014).

95) Hayyan, M.; Mjalli, F. S.; Hashim, M. A.; AlNashef, I. M. & Mei, T. X., Investigating the electrochemical window of ionic liquids. *J. Indust. Eng. Chem*. **19**, 106-112 (2013).

96) Tiago, G. A. O.; Matias, I. A. S.; Ribeiro, A.P. C.& Martins, L. M. D. R. S., Application of Ionic Liquids in Electrochemistry – Recent Advances. *Molecules*, **25**, 5812 (2020).

97) Sedev, R., Surface tension, interfacial tension and contact angles of ionic liquids. *Curr. Opin. Coll. Interface Sci.* **16**, 310-316 (2011).

98) Kamlet, M. J., Abboud, J. L. M., Abraham, M. H & Taft, R. W. Linear Solvation Energy Relationships. 23. A Comprehensive Collection of the Solvatochromic Parameters, p*, a, and ß, and Some Methods for Simplifying the Generalized Solvatochromic Equation. *J. Org. Chem.* **48**, 2877-2887 (1983).

This work sets out the parameters used to describe solvents and is a useful resource bringing together the numerical values for a range of different solvents.

99) Black, A. W. & Bartlett, P. N., Selection and characterisation of weakly coordinating solvents for semiconductor electrodeposition. *Phys. Chem. Chem. Phys*. **24**, 8093-8103 (2022).

100) Bartlett, P. N. *et al*, A Versatile Precursor System for Supercritical Fluid Electrodeposition of Main-Group Materials. *Chem. Eur. J.* **22**, 302-309 (2016).

101) Fan, L. & Suni, I. I., Electrodeposition and Capacitance Measurements of WS_2 Thin Films, *J. Electrochem. Soc.* **164**, D681-D686 (2017).

102) Bartlett, P. N. *et al*, Non-aqueous electrodeposition of functional semiconducting metal chalcogenides: $Ge_2Sb_2Te_5$ phase change memory. *Mater. Horiz.* **2**, 420-426 (2015).

    This work describes a method for the electrodeposition of GeSbTe thin films and nanostructures from a CH_2Cl_2 electrolyte using compatible multi-source precursors

103) Kissling, G. P. *et al*, Electrodeposition of a Functional Solid State Memory Material: Germanium Antimony Telluride from a Non-Aqueous Plating Bath. *J. Electrochem. Soc.* **165**, D557-D567 (2018).

104) Bartlett, P. N. *et al*, Non-aqueous electrodeposition of p-block metals and metalloids from halometallate salts. *RSC Adv.* **3**, 15645-15654 (2013).

105) Lodge, A. W. *et al*, Electrodeposition of tin nanowires from a dichloromethane based electrolyte. *RSC Adv.* **8**, 24013-24020 (2018).

106) Bartlett, P. N. *et al*, Haloplumbate salts as reagents for the non-aqueous electrodeposition of lead. *RSC Adv.* **6**, 73323-72330 (2016).

107) Cook, D. A., Reeves, S. J., Zhang, W., Reid, G., Levason, W. & Bartlett, P. N., Cathodic stripping of elemental Te in dichloromethane, *Electrochim. Acta*, **465**, 142997 (2023).

108) Bartlett, P. N., Cummings, C. Y., Levason, W., Pugh, D. & Reid, G., Halometallate Complexes of Germanium(II) and (IV): Probing the Role of Cation, Oxidation State and Halide on the Structural and Electrochemical Properties, *Chem. Eur. J.* **2**, 5019-5027 (2014).

109) Evans, D. H., One-electron and Two-Electron Transfers in Electrochemistry and Homogeneous Solution Reaction. *Chem. Rev.* **108**, 2113-2144 (2008).

110) Cicvaric, K. *et al*, Thermoelectric Properties of Bismuth Telluride Thin Films Electrodeposited from a Nonaqueous Solution. *ACS Omega*, **5**, 14679-14688 (2020).

111) Jaafer, A. H. *et al*, Flexible Memristor Devices Using Hybrid Polymer/Electrodeposited GeSbTe Nanoscale Thin Films. *ACS Appl. Nano Mater*. **5**, 17711–17720 (2022).

112) Noori, Y. J. *et al*, Phase-Change Memory by GeSbTe Electrodeposition in Crossbar Arrays. *ACS Appl. Electron. Mater*. **3**, 3610-3618 (2021).

113) Liang, T. *et al*, A facile approach to enhance the hydrogen evolution reaction of electrodeposited MoS_2 in acidic solutions. *New J. Chem.* **46**, 23344-23350 (2022).

114) Xue, J. *et al*, Enhanced photoelectrocatalytic hydrogen production performance of porous MoS_2/PPy/ZnO film under visible light irradiation. *Int. J. Hydr. Energy*, **46**, 35219-35229 (2021).

115) Nisar, T., Balster, T. & Wagner, V., Mechanical transfer of electrochemically grown molybdenum sulfide layers to silicon wafer. *J. Appl. Electrochem.* **51**, 1279–1286 (2021).

116) Aslan, E. & Patir, I. H., Catalysis of hydrogen evolution reaction by *in situ* electrodeposited amorphous molybdenum sulfide at soft interfaces. *Mater. Today Energy*, **21**, 100742 (2021).

117) Chakraborty, B., Maity, I., Chung, P., Ho, M. & Bhattacharyya, P., Understanding the Highly Selective Methanol Sensing Mechanism of Electrodeposited Pristine MoS_2 Using First Principle Analysis, *IEEE Sensors J*. **21**, 15 (2021).

118) Shit, S., Bolar, S., Murmu, N. C. & Kuila, T., Tailoring the bifunctional electrocatalytic activity of electrodeposited molybdenum sulfide/iron oxide heterostructure to achieve excellent overall water splitting, *Chem. Eng. J.,* **417**, 129333 (2021).

119) Levinas, R., Tsyntsaru, N. & Cesiulis, K., The Characterisation of Electrodeposited MoS_2 Thin Films on a Foam-Based Electrode for Hydrogen Evolution. *Catalysts,* **10**, 1182 (2020).

120) Chang, C.-Y., Anuratha, K. S., Lin, Y.-H., Xiao, Y., Hasin, P. & Lin, J.-Y., Potential-reversal electrodeposited MoS_2 thin film as an efficient electrocatalytic material for bifacial dye-sensitized solar cells. *Sol. Energy.* **206**, 163-170 (2020).

121) Yagati, A. K., Go, A., Vu, N. H. & Lee, M. H., A MoS_2–Au nanoparticle-modified immunosensor for T_3 biomarker detection in clinical serum samples. *Electrochim. Acta,* **342**, 136065 (2020).

122) Gurulakshmi, M. *et al*, Electrodeposited MoS_2 counter electrode for flexible dye sensitized solar cell module with ionic liquid assisted photoelectrode. *Sol. Energy*, **199**, 447-452 (2020).

123) Lei, Y. *et al*, Synthesis of V-MoS_2 Layered Alloys as Stable Li-Ion Battery Anodes. *ACS Appl. Energy Mater.* **2**, 8625–8632 (2019).

124) Giang, H., Pali, M., Fan, L. & Suni, I. I., Impedance Biosensing atop MoS_2 Thin Films with Mo−S Bond Formation to Antibody Fragments Created by Disulphide Bond Reduction. *Electroanal.* **31**, 957-965 (2019).

125) Yang, L. *et al*, Efficient hydrogen evolution catalyzed by amorphous molybdenum sulfide/N-doped active carbon hybrid on carbon fiber paper. *Int. J. Hydr. Energy*, **43**, 15135-15143 (2018).

126) Amin, R., Hossain, M. A. & Yahya Zakaria, Y., Interfacial Kinetics and Ionic Diffusivity of the Electrodeposited MoS_2 Film. *ACS Appl. Mater. Interfaces*, **10**, 13509–13518 (2018).

127) Chia, X., Sutrisnoh, N. A. A & Pumera, M., Tunable Pt–MoS_x Hybrid Catalysts for Hydrogen Evolution, *ACS Appl. Mater. Interfaces,* **10**, 8702–8711 (2018).

128) Lamouchi, A., Assaker, I. B. & Chtourou, R., Effect of annealing temperature on the structural, optical, and electrical properties of MoS_2 electrodeposited onto stainless steel mesh. *J. Mater. Sci*. **52**, 4635–4646 (2017).

129) Falola, B. D., Wiltowski, T. & Suni, I. I., Electrodeposition of MoS_2 for Charge Storage in Electrochemical Supercapacitors. *J. Electrochem. Soc.* **163,** D568 (2016).

130) Ahn, H. S. & Bard, A. J., Electrochemical Surface Interrogation of a MoS_2 Hydrogen-Evolving Catalyst: In Situ Determination of the Surface Hydride Coverage and the Hydrogen Evolution Kinetics. *J. Phys. Chem. Lett.* **7**, 2748–2752 (2016).

131) Ponomarev, E. A., Tenne, R., Katty, A. & Lévy-Clément, C., Highly oriented photoactive polycrystalline MoS_2 layers obtained by van der Waals rheotaxy technique from electrochemically deposited thin films. *Sol. Energy Mater. Sol. Cells,* **52**, 125-133 (1998).

132) Albu-Yaron, A., Lévy-Clément, C., Katty, A., Bastide, S. & Tenne, R., Influence of the electrochemical deposition parameters on the microstructure of MoS_2 thin films. *Thin Solid Films,* **361–362**, 223-228 (2000).

133) Ponomarev, E. A., Albu-Yaron, A., Tenne, R. & Lévy-Clément, C., Electrochemical Deposition of Quantized Particle MoS_2 Thin Films. *J. Electrochem. Soc.* **144**, L277 (1997).

134) Fan, L. & Suni, I. I., Polysulfide Reduction and Oxidation at MoS_2, WS_2 and Cu-Doped MoS_2 Thin Film Electrodes. *J. Electrochem. Soc.* **166,** A1471 (2019).

135) Novčić, K. A., Iffelsberger, C., Ng, S. & Pumera, M., Local electrochemical activity of transition metal dichalcogenides and their heterojunctions on 3D-printed nanocarbon surfaces. *Nanoscale*, **13**, 5324-5332 (2021).

136) Pu, Z., Liu, Q., Asiri, A. M., Obaid, A. Y., Sun, X., One-step electrodeposition fabrication of graphene film-confined WS_2 nanoparticles with enhanced electrochemical catalytic activity for hydrogen evolution. *Electrochim. Acta,* **134**, 8-12 (2014).

137) Redman, D. W., Rose, M. J., Stevenson, K. J., Electrodeposition of Amorphous Molybdenum Chalcogenides from Ionic Liquids and Their Activity for the Hydrogen Evolution Reaction. *Langmuir*, **33**, 9354-9360 (2017).

138) Ng, S., Iffelsberger, C., Sofer, Z, & Pumera, M. Tunable Room-Temperature Synthesis of ReS_2 Bicatalyst on 3D- and 2D-Printed Electrodes for Photo- and Electrochemical Energy Applications. *Adv. Funct. Mater*. **30**, 1910193 (2020).

139) Wallace, A. G. *et al*, Anodic Sb_2S_3 electrodeposition from a single source precursor for resistive random-access memory devices. *Electrochim. Acta,* **432**, 141162 (2022).

140) Thomas, S. *et al*, Electrodeposition of MoS_2 from Dichloromethane, *J. Electrochem. Soc*. **167**, 106511 (2020).

141) Thomas, S. *et al*, Tungsten disulfide thin films *via* electrodeposition from a single source precursor. *Chem. Commun*. **57**, 10194-10197 (2021).
This work describes the preparation and electrochemistry of a stoichiometric SSP for the electrodeposition of WS_2 without the need for a proton source.

142) O'Neal, S. C. & Kolis, J. W., Convenient Preparation and Structures of Selenometalates $MoSe_4^{2-}$, WSe_4^{2-}, and $MoSe_9^{2-}$ from Polyselenide Anions and Metal Carbonyls. *J. Am. Chem. Soc*. **110**, 1971-1973 (1988).

143) Kim, J. *et al*, A facile synthetic route to tungsten diselenide using a new precursor containing a long alkyl chain cation for multifunctional electronic and optoelectronic applications. *RSC Adv*. **9**, 6169–6176 (2019).

144) Klingelhöfer, P. & Müller, U., Thiochlorowolframate von Wolfram(V) und -(VI). Die Kristallstrukturen von $PPh_4[WSCl_4]$ und $(PPh_4)_2[WS_2Cl_4]\cdot 2CH_2Cl_2$. *Z. Anorg. Allg. Chem*. **556**, 70–78 (1988).

145) Greenacre, V. K., Hector, A. L., Huang, R., Levason, W., Sethi. V. & Reid, G., Tungsten(VI) selenide tetrachloride, $WSeCl_4$ – synthesis, properties, coordination complexes and application of $[WSeCl_4(Se^nBu_2)]$ for CVD growth of WSe_2 thin films. *Dalton Trans.* 51, 2400-2412 (2022).

146) Thomas, S. *et al*, University of Southampton, unpublished work.

147) Das, S. *et al*, A Self-Limiting Electro-Ablation Technique for the Top-Down Synthesis of Large-Area Monolayer Flakes of 2D Materials. *Sci. Rep.* **6**, 28195 (2016).

This article describes a method for electropolishing multilayer (bulk) TMDC crystals to produce monolayers.

148) Wan, X. *et al*, Controlled Electrochemical Deposition of Large-Area MoS_2 on Graphene for High-Responsivity Photodetectors. *Adv. Funct. Mater*. **27**, 1603998 (2017).

149) Noori, Y. J. *et al*, Large-Area Electrodeposition of Few-Layer MoS_2 on Graphene for 2D Material Heterostructures, *ACS Appl. Mater. Interfaces,* **12**, 49786–49794 (2020).

150) Noori, Y. J. *et al*, Electrodeposited WS_2 monolayers on patterned graphene, *2D Mater*. **9**, 015025 (2022).

The article describes a method for the electrochemical growth of ultra-thin WS_2 over graphene electrodes using a SSP and a dichloromethane electrolyte.

151) Abdelazim, N. *et al*, Lateral Growth of MoS_2 2D Material Semiconductors Over an Insulator Via Electrodeposition. *Adv. Electron. Mater.* **7**, 2100419 (2021).

This article describes the clean-room fabrication process for nano-band electrodes and their application for the electrochemical growth of 2D MoS_2 over an insulating SiO_2 surface.

152) Greenacre, V. K., Levason, W., Reid, G. & Smith, D. E. Coordination complexes and applications of transition metal sulfide and selenide halides. *Coord. Chem. Rev.* **424**, 213512 (2020).

153) Black, A. W., Zhang, W., Noori, Y. J., Reid, G. & Bartlett, P. N., Temperature effects on the electrodeposition of semiconductors from a weakly coordinating solvent. *J. Electroanal. Chem.* **944**, 117638 (2023).

154) Liang, X., Jayaraju, N., Thambidurai, C., Zhang, Q. and Stickney, J. L., Controlled Electrochemical Formation of $Ge_xSb_yTe_z$ using Atomic Layer Deposition (ALD), *Chem. Mater*. **23**, 1742–1752 (2011).

155) Schwarzacher, W. and Lashmore, D. S., Giant Magnetoresistance in Electrodeposited Films, *IEEE Trans. Magnetics*, **32**, 3133-3153 (1996).

156) Jyoko, Y. and Schwarzacher, W., Characterization of electrodeposited magnetic Co/Pt multilayered nanostructures, *Electrochim. Acta*, **47**, 371-378 (2001).

Tables:

Table 1. The Taft solvent descriptors for some commonly used electrochemical solvents, together with those for the weakly coordinating CH_2Cl_2 (π^*, α and β describe the polarity, Lewis acidity and Lewis basicity, respectively).[98,99] Suitable solvents typically have $\pi^* \geq 0.55$, $\alpha \leq 0.2$, and $\beta \leq 0.2$.

Solvent	π^*	α	β
MeCN	0.75	0.19	0.4
DMSO	1.00	0	0.76
Ethylene glycol	0.92	0.90	0.52
CH_2Cl_2	0.82	0.13	0.01

Figure captions

Figure 1: Crystal structure of a 2D layered transition metal dichalcogenide (TMDC). a) an edge-view of the structure in a tri-layer with the layer dimensions; b) the octahedral and trigonal prismatic stacking arrangements present in different TMDC polytypes (blue = metal; green = chalcogen).

Figure 2 Schematic showing a typical three-electrode electrochemical cell set-up for electrodeposition. (a) the three-electrode set-up showing the potentiostat that controls the potential between the working electrode (WE) and the reference electrode (RE) while recording the current that flows between the WE and counter electrode (CE). The RE acts as a fixed, reproducible, point against which to apply, or measure, the potential at the working electrode. This allows precise control over the driving force for electrodeposition. The three-electrode system can be used to carry out different experiments, including (b) macroelectrode cyclic voltammetry, (c) microelectrode voltammetry, and (d) rotating disc voltammetry. In all three techniques the potential of the working electrode is scanned back and forth at a constant rate and the current recorded. This enables the study and characterisation of the electrodeposition chemistry, the electrode reactions of the precursor, and the different processes (electron transfer, mass transfer, coupled solution chemical reactions, surface and adsorption processes, *etc*.) involved (see Ref. 54 for details). Negative currents in (b), (c) and (d) correspond to the deposition of material on the working electrode by reduction of the precursor in solution. Positive currents, on the return scan to positive potentials, correspond to stripping (oxidation) of the deposited material from the working electrode surface. The three-electrode system can also be used to follow the electrodeposition current as a function of time (e). The amount of material deposited on the working electrode can be controlled, or monitored, by following the total charge passed and using Faraday's law of electrolysis. (The plotted curves (b to e) are taken from

1038 experimental results for deposition of Sb from $[SbCl_4]^-$ in CH_2Cl_2 containing $[N^nBu_4]Cl$ electrolyte in Ref.
1039 55).

1040 **Figure 3** The molecular species involved in the deposition of elemental tellurium from reduction of
1041 $[TeCl_6]^{2-}$. (a) process involved in the reversible dissociation of Cl^- (green spheres) from the $[TeCl_6]^{2-}$
1042 precursor in CH_2Cl_2, to give the Lewis acidic $[TeCl_5]^-$ anion with a vacant coordination site (grey orbital
1043 lobe); (b) a schematic showing a $[TeCl_5]^-$ anion bonding to the Lewis basic electrodeposited Te^0 surface
1044 (orange spheres = Te) *via* interaction with a *p*-type orbital orthogonal to the growing surface. Redrawn
1045 from Ref. 47.

1046

1047 **Figure 4** Illustrating a multi-source precursor approach for the electrodeposition of ternary
1048 germanium antimony telluride alloys. (a) the structures of the three precursor anions, $[GeCl_5]^-$, $[SbCl_4]^-$
1049 and $[TeCl_6]^{2-}$; (b) a cyclic voltammogram (CV) recorded from the electrolyte containing these three
1050 chlorometallate ions in CH_2Cl_2 solution and containing $[N^nBu_4]Cl$ supporting electrolyte – from Ref.
1051 102. The peaks corresponding to the reduction processes for each of the three reagents are labelled.

1052

1053 **Figure 5** Examples of single source precursors (SSPs) used for 2D-TMDC electrodeposition. (a) the
1054 $[ME_4]^{x-}$ anions,;(b) the preparation methods for $[WECl_4]$ (E = S or Se) and the $[WS_2Cl_4]^{2-}$ anion.

1055 **Figure 6** Illustration of 2D- TMDC electrodeposition over a conductor (electrode). (a) Schematic
1056 showing the growth of a TMDC 2D layer onto a graphene electrode; (b) the fabrication process used
1057 to produce the microelectrodes; (c) transmission electron microscopy (TEM) image of a WS_2
1058 monolayer deposited onto graphene using the electrode structure in (a) – from Ref. 150.

1059

1060

1061 **Figure 7** Schematic showing anisotropic growth of 2D-TMDCs from the edges of nano-band electrodes
1062 over an insulator (SiO_2). (a) concept diagram showing the 2D layer growing only from the exposed
1063 edges of the TiN nano-band electrode; (b) a TEM image showing an electrodeposited MoS_2 tri-layer
1064 grown using the electrode structure in (c), where MoS_2 is grown from the TiN band electrodes on both
1065 the left (TMDC-1) and right (TMDC-2); (c) illustration of the fabrication process steps (i) to (v) for the
1066 nano-band electrodes; (d) The design principle of a chip where micro-gap nano-band electrodes can
1067 enable 2D TMDC electrodeposition over an insulator; (e) and (f) show low and high magnification
1068 microscope images of the micro-gap electrode arrays with TMDCs (blue) grown between the
1069 electrodes. Redrawn from Ref. 151.

1070

1071

1072 **Glossary**

1073 area-selective growth   materials growth only on specific regions of a pre-patterned substrate

1074 anisotropic growth   growth strongly favoured in one or two specific direction(s); in the case of
1075   TMDCs, this is typically from the edges of the growing layer (to produce a
1076   2D sheet)

1077 microelectrodes   an electrode with diameter < 50 μm

1078 macroelectrodes   an electrode with diameter > 0.1 mm

1079 SSP   single source precursor; a compound that can be used for depositing the target TMDC
1080   and containing pre-formed metal-chalcogen bonds

1081 electrolyte   the solution used for the electrochemical experiment, usually comprising the solvent,
1082   precursor(s) and a redox inactive cation-anion salt that dissociates in the solvent to
1083   form ions that carry the charge

1084 nano-band electrode   an electrode structure where the conducting surface is in the form of a line
1085   < 100 nm deep, typically fabricated on a silicon substrate

1086 brightener   a chemical used in electrodeposition to increase the optical brightness of the deposited
1087   material

1088 leveller   a chemical used in electrodeposition to increase the uniformity of the deposited
1089   material

1090 counter electrode   the electrode used to complete the circuit in the electrochemical cell. It has
1091   to pass an equal but opposite current from that at the working electrode

1092 planar diffusion   diffusion in 1D to/from the electrode surface

1093 radial diffusion   diffusion in 2D or 3D to/from the electrode surface

1094 *iR* drop   difference between the applied potential and the potential at the working
1095   electrode due to passage of current through solution, or other
1096   uncompensated resistance.

Short summary

Electrochemical methods to grow 2D metal chalcogenides are reviewed, emphasising the effects of the precursor(s), solvent and electrode designs. Emerging work using nano-band electrodes to promote in-plane 2D layer growth into 'device-ready' electrode structures is highlighted.

33